Novel Technology for Facial Muscle Stimulation Combined With Synchronized Radiofrequency Induces Structural Changes in Muscle Tissue: Porcine Histology Study

Brian M. Kinney, MD, FACS; Jan Bernardy, MVDr, PhD; and Rea Jarošová, MSc, PhD

Aesthetic Surgery Journal
2023, Vol 43(8) 920–927

https://doi.org/10.1093/asj/sjad053
www.aestheticsurgeryjournal.com

OXFORD
UNIVERSITY PRESS

Abstract

Background: With age, facial muscles lose the ability to complete contractions properly, resulting in limitation of facial expressions and fat shifting, and leading to skin creases and wrinkling.

Objectives: The aim of this study was to determine the effects of the novel high intensity facial electromagnetic stimulation (HIFES) technology combined with synchronized radiofrequency on delicate facial muscles, using an animal porcine model.

Methods: Eight ($n = 8$, 60-80 kg) sows were divided into the active group ($n = 6$) and the control group ($n = 2$). The active group underwent four 20-minute treatments with radiofrequency (RF) and HIFES energies. The control group was not treated. Histology samples of muscle tissue were collected by a punch biopsy (6 mm in diameter) from the treatment area of each animal at baseline, 1-month, and 2-month follow-up. The evaluation included staining of the obtained tissue slices with hematoxylin and eosin and Masson's trichrome to determine the changes in muscle mass density, number of myonuclei, and muscle fibers.

Results: The active group showed muscle mass density increase (by 19.2%, $P < .001$), together with elevated numbers of myonuclei (by 21.2%, $P < .05$) and individual muscle fibers, which increased from 56.8 ± 7.1 to 68.0 ± 8.6 ($P < .001$). In the control group, no significant changes were seen in any of the studied parameters throughout the study ($P > .05$). Finally, no adverse events or side effects were observed in the treated animals.

Conclusions: The results document favorable changes after the HIFES + RF procedure at the level of the muscle tissue, which may be of great importance in terms of maintenance of facial appearance in human patients.

Editorial Decision date: February 28, 2023; online publish-ahead-of-print March 8, 2023.

Aging is a multifactorial process that affects all body structures, causing emotional distress through altering of the visual appearance and thus self-perception.[1–3] In the face, the skeleton, ligaments, muscles, adipose tissue, and skin undergo age-related changes at a different pace, however all structures interact with each other. Therefore, changes in one structure affect others.[4] Facial muscles are one of the most affected structures. Muscle changes can be promoted by age and gradually lose their mass and function after the third decade of life.[5] The imbalance between the degradation and synthesis of new muscle fibers leads to functional setbacks, recognized as sarcopenia.[6] Atrophic changes in the muscle tissue can also result from neuromodulators such as botulinum toxin type A injections.[7,8] The deconditioned muscles manifest themselves with loss of strength, disorganized sarcomere spacing, and decrease in plasma

Dr Kinney is a clinical associate professor of plastic surgery, USC Keck School of Medicine, Los Angeles, CA, USA. Drs Bernardy and Jarošová are clinical researchers, Veterinary Research Institute, Brno, Czech Republic.

Corresponding Author:
Dr Jan Bernardy, Veterinary Research Institute, Hudcova 296/70, 621 00 Brno, Czech Republic.
E-mail: bernardyj@gmail.com; Instagram: @bernardyjan

membrane excitability, all of which lead to decreased muscle twitch time and twitch force.[5,6] Because the facial structures are intertwined, changes in one structure can manifest themselves in other structures, and as a result of this deterioration in muscle function certain facial expressions may be limited, and changes in adjacent structures can be seen as well, such as fat shifting and skin wrinkling.[4]

Facial muscles are a type of striated muscles that (in contrast to skeletal counterparts, which facilitate movement of entire body parts) are embedded in a connective tissue framework that interconnects all tissues from bone to skin to perform facial emotional expressions and mastication.[9] Recently high-intensity focused electromagnetic (HIFEM) technology synchronized with radiofrequency (RF) has been proven to be safe and effective in muscle strengthening of the large skeletal muscle groups; however, due to the physiological differences between skeletal and facial muscles, novel high intensity facial electromagnetic stimulation (HIFES) technology with synchronized radiofrequency was developed to strengthen delicate facial muscles to combat the signs of aging.[1,10–12] Regarding muscle action, there is a substantial difference between voluntary and induced muscle contractions. The general mechanism of voluntary muscle contraction starts with a signal from the brain—an action potential. It is essentially an electrical impulse that travels through the motor neuron to the synapses (neuromuscular junction), releasing the neurotransmitter and influencing the membrane's electrical potential, causing depolarization and activation of muscle contraction, followed by the relaxation phase.[13,14] The novel HIFES technology, however, induces so-called supramaximal contractions independent of brain activity. Moreover, due to the tailored stimulation frequency, the muscle contractions are considerably intensified because the relaxation phase does not follow every single stimulus. The synchronized RF aids the effect of the HIFES field by heating the muscle tissue within a safe range of temperatures (below 42°C), activating protein synthesis and increasing the expression of heat-shock proteins, which help with muscle regeneration and growth.[15,16] Additionally, RF heating leads to neocollagenesis and neoelastinogenesis, creating firm, tightened, lifted, and smooth skin.[17]

The HIFES technology synchronized with radiofrequency has the potential to treat the vast majority of facial imperfections because it is able to target both muscle and connective tissues. However, the aim of this animal histology study is to investigate its effects and safe use on muscle remodeling, focusing on the structural organization of this tissue.

METHODS

This prospective, single-center animal study was approved by the Institutional Animal Care and Use Committee and the Ethics Committee for Animal Protection of the Ministry of Agriculture of the Czech Republic. The study was initiated in June 2021 and was completed in September 2021. It was performed in association with and supervised by a veterinary institute certified for good laboratory practice. All animals were stabled at the veterinary institute, so the veterinarian and veterinary staff handled the animal care to ensure animal welfare during the study. After performing all the planned procedures and collection of all samples, the animals were euthanized by an analgesic overdose (T61 a.u.v. inj, Intervet International B.V./MSD AH, Boxmeer, the Netherlands) administered by a veterinarian.

Animal Model and Treatment Settings

Eight large white pigs ($n = 8$ females, 60-80 kg of live weight) were utilized for this trial. Six sows ($n = 6$, active group) underwent four 20-minute treatments on the forehead once a week with simultaneous application of HIFES and RF. Two sows ($n = 2$, control group) were not treated. The control group was established to reduce the number of punch biopsies taken from the treated animals and to allow them to heal properly. In addition, all treated animals had blood tests and were examined to ensure their health and to rule out any possibility of unexpected interference with results. The treatments were delivered by noninvasive self-adhesive, hands-free EMFACE applicators (BTL Industries, Boston, MA) emitting both RF and HIFES energies and covering approximately 53 cm^2 (Figure 1). Both energies were set at 100% intensity. In addition, optical fiber sensors were inserted into the treated muscles under the applicator (LumaSense Flurotropic Thermometer; Lumasense Technologies, Santa Clara, CA) to monitor the temperature during the treatment. An infrared camera measured the skin temperature immediately after the treatments (Fluke Ti300; Fluke Corporation, Everett, WA).

During the treatment and collection of punch biopsies, the animals were kept under general anesthesia for easier manipulation and comfort. At first, the premedication for anesthesia consisting of Tiletamine + Zolazepam (Zoletil 100 Virbac; Carros, France) + Ketamine (Narketan, Vetoquinol; Lure Cedex, France) + Xylazine (Sedazine, Fort Dodge; Overland Park, KS), each medicine dosed at 2 mg/kg, was administered intramuscularly. Then, an intravascular cannula was placed into the ear's vein to infuse propofol 2% MCT/LCT (Fresenius; Bad Homburg, Germany), dosed at 1-2 mg/kg to maintain anesthesia. The animal's heart activity was monitored by electrocardiogram. A certificated veterinarian oversaw the animals during the entire treatment sessions and follow-ups, including assessment of adverse events and side effects related to the study device.

Three samples of muscle tissue per animal were collected by a punch biopsy (6 mm in diameter) taken from the treatment area on the forehead (active group) and a corresponding place on the forehead of those in the control

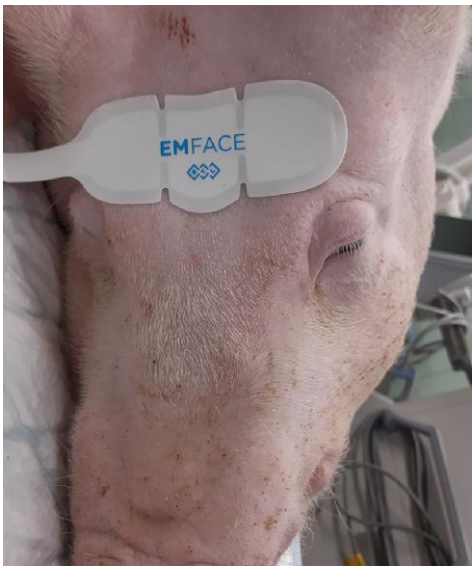

Figure 1. Visualization of the self-adhesive, hands-free EMFACE applicator intended to treat the forehead area in human patients.

group. All samples were collected in the anesthetized animals before the first treatment, and at 1-month and 2-month follow-ups, to minimize the suffering of the sows. After the sampling procedure, the wound was disinfected, closed with 2 clamps, and covered with an adhesive bandage to protect the wound from infection.

Evaluation of Muscle Changes

Each muscle sample was stored in a container with 10% neutral buffered formalin (in a sample-to-fixative ratio of approximately 1:30) to preserve the tissue condition at the time of collection. The samples were then embedded in paraffin wax, sliced on the microtome, and stained with hematoxylin and eosin (H&E) and with Masson's trichrome for visualization in longitudinal and transverse cross-sections.

The hematoxylin has to be oxidized into hematein to gain staining abilities, and because it is positively charged it dyes the nucleus in a dark-blue color.[18,19] The eosin is negatively charged and stains the proteins and cytoplasm pink.[20] The staining process starts with immersing the slides in H_2O to clean the formalin and rehydrate the samples. Then, the slides are dyed with hematoxylin, rinsed, and stained with eosin. Next, the dyed sample is dehydrated with alcohol because some substances can be better dissolved. Then the alcohol is rinsed again, and the sample is mixed with a mounting medium and covered with a coverslip.[20] The muscle cells consist of myofilaments and intermediate filaments in the cytoplasm, which after H&E staining appear deep pink, with multiple nuclei dyed in dark blue color, allowing analysis of the morphology of each structure.[19,21]

Masson's trichrome staining consists of 3 dyes, a Weigert hematoxylin that stains the nucleus (dark brown), an acid stain (Ponceau–Fuschin) which stains muscle fibers (red), and a phosphotungstic acid (orange G), a decolorizing agent, which diffuses out of the collagen fiber while leaving the muscle cells stained red.[22–24] Additionally, Goldner's stain III (light green SF yellowish) dye was utilized to stain collagen fibers green and erythrocytes orange.[22,25] The staining process starts with refixing the samples in Bouin solution, which improves the quality of the stain. The slide is rinsed with tap water and stained with Weigert hematoxylin and again rinsed with tap and distilled water. Then it is dyed with an acid stain, rinsed with distilled water, immersed in phosphotungstic acid, and stained with Goldner's stain III. At this point, the sample is rinsed in distilled water and differentiated with 1% acetic acid, washed again in distilled water, dehydrated with alcohol, and cleaned with xylene. The last step is to mount the sample with a mounting medium and cover it with the coverslip.[22]

All stained slices were then visualized under a light microscope and photographed with Hitachi Axio Scan.Z1 (Carl Zeiss AG; Oberkochen, Germany) with a 20×/0.8NA Plan-Apochromat objective. The primary outcome measures included calculating muscle mass, the number of myonuclei located on the periphery of the sectioned muscle fibers, the number of muscle fibers, and the diameter of individual muscle fibers. The evaluation was performed with semiautomatic processing and analytic software ImageJ (National Institutes of Health; Bethesda, MD) in the predefined regions of interest (ROI) of 122,500 μm^2.

The descriptive statistic was calculated (mean, standard deviation) when analyzing the obtained quantitative data. To determine the statistical significance of the changes the Friedman test, followed by the Nemenyi test, for pairwise comparisons was performed. In addition, a Wilcoxon rank sum test was done to compare independent data. For all statistical analyses, the significance level of α=.05 was set.

RESULTS

All animals recovered from the anesthesia without any complications. No treatment-related side effects were observed in any of the animals or on the histological evaluation. In total, 24 muscle samples were collected during the study period, with each sample sliced, stained (3 slices per each staining, 144 slices in total), and evaluated to determine the primary outcomes. In general, there was no difference between the groups (P value > .05) in any of the measured outcomes at baseline. However, as the study progressed, the active group showed significant changes at the follow-ups and when compared with the control group. The temperature measurements revealed elevated

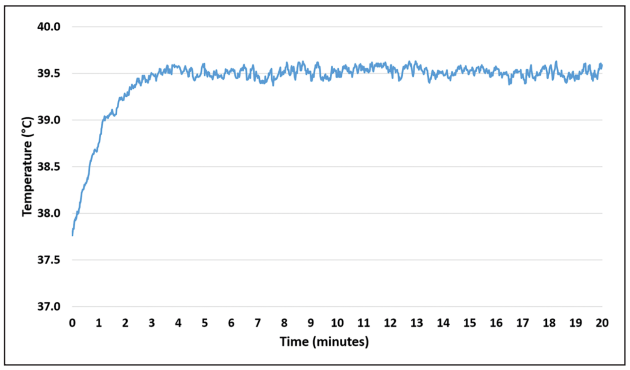

Figure 2. The temperature development in the muscle tissue during the therapy. The temperature rises to 39.5°C within 2 minutes and stays essentially unchanged for the rest of the therapy time.

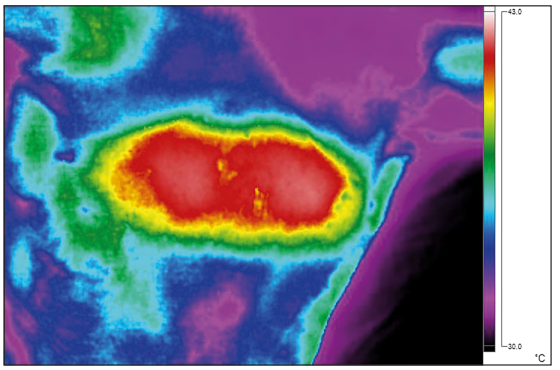

Figure 3. The skin temperature measurements were taken immediately after the treatment. The maximum surface temperature in the treatment area was just above 42°C, not exceeding 42.5°C. A thermal image taken by an infrared camera Fluke Ti300 (Fluke Corporation; Everett, WA).

muscle temperature from the onset of therapy, exceeding the 39°C within 2 minutes and stabilizing at the level of approximately 39.5°C in the third minute of therapy (Figure 2). The skin temperature measurements showed safe values at the level of 42°C (Figure 3).

The Evaluation of Muscle Mass

In the active group, the average muscle area in the ROI was 60810.1 μm^2 at baseline. At a 1-month follow-up visit, the average muscle area had significantly increased to 69223.2 μm^2 (P value = .003). Finally, the increase peaked at a 2-month follow-up visit with the average muscle area being 72474.4 μm^2 (P value < .001). Compared to baseline, the average muscle density was increased by 13.8% at 1 month and 19.2% at the 2-month follow-up visit in the active group. The observed changes in the examined histology slices are visualized in Figures 4, 5. In the control group, the baseline muscle area was 61711.4 μm^2 and did not show any substantial changes during the 1-month (61455.6 μm^2, P value > .05) or 2-month (62076.1 μm^2, P value > .05) follow-up.

The Number of Myonuclei

The average number of nuclei in the active group increased from 146.6 ± 24.9 (baseline) to 161.7 ± 26.7 (10.3% increase) at the 1-month follow-up visit, and up to 177.7 ± 30.7 (21.2% increase) at 2-month follow-up. The changes were significant at both follow-up visits (P value < .05). In the control group, however, the change in the nuclei count was insignificant (P value = .75 at 1 month; P value = .57 at 2 months), because it rose slightly from 136.7 ± 21.7 (baseline) to 140.3 ± 20.4 at 1 month and stayed at 140.3 ± 18.8 at 2 months.

The Number and Size of Muscle Fibers

In the active group, the average number of fibers in the ROI was 56.8 ± 7.1 at baseline, gradually increasing to 62.5 ± 9.2 fibers (10.1% increase, P value = .03) at 1-month follow-up. Analogous to the muscle density and myonuclei, the fiber count peaked at a 2-month follow-up visit with 68.0 ± 8.6 fibers (19.8% increase, P value < .001) per ROI. In the control group, the number of fibers was 56.3 ± 6.5 at baseline, with little to no increase throughout the study (57.3 ± 9.6 at 1 month, P value = .48; 58.2 ± 6.7 at 2 months, P value = .32). The changes in the number of muscle fibers compared with the control group were significant at the 2-month follow-up (P value = .004).

The increase in the diameter of the muscle fibers was visible in the active group throughout the study period. At baseline, the average muscle fiber size was 32.6 ± 2.5 μm, with a size of 33.6 ± 2.3 μm at 1-month follow-up and 37.8 ± 5.3 μm at 2 months (P value < .05). In the control group, no significant changes were observed (P value > .05), because the average muscle fiber size was 32.5 ± 0.31 μm throughout the study. The change in the relative frequency distribution of measured fibers can be seen on the histogram in Figure 6. Results indicate that the number of small-sized fibers considerably decreased over the course of the study. At the same time, there were increased numbers of thicker muscle fibers in follow-up samples from the active group. The histogram shows that the most common fiber size per ROI was between 30-40 μm in diameter at baseline. At the follow-ups, the number of fibers with a diameter greater than 40 μm was most abundant in the ROI.

DISCUSSION

In this study we evaluated the effects of novel HIFES technology combined with synchronized RF on deconditioned

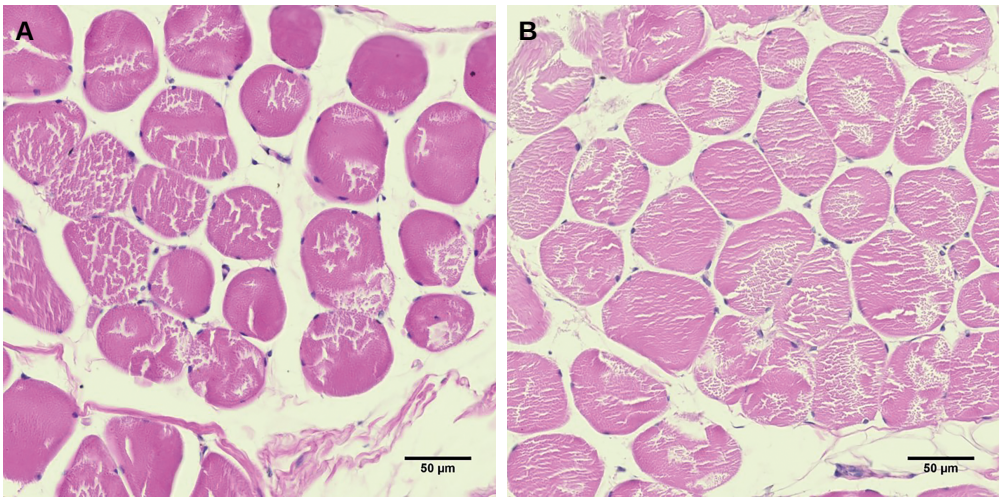

Figure 4. A cross-sectional view of the muscle tissue in the active group stained by hematoxylin and eosin, taken at (A) baseline and (B) 2-month follow-up. The pink represents the muscle tissue with dark purple nuclei at the periphery. The muscle tissue is noticeably denser after treatments in the assessed regions of interest.

muscle tissue. Based on the data obtained, we observed a consistent and significant increase in all studied parameters related to the quality and function of the muscle tissue. During the study, no treatment-related issues or side effects were observed in any of the animals or histological samples. The measured temperatures in the muscle tissue as well as on the surface showed that the heat was within the safe but effective limits. The results indicated that the simultaneous application of HIFES + RF safely and effectively targets the muscle tissue while promoting muscle remodeling and structural improvement.

Facial muscles are subject to the ravages of time together with the rest of the body tissues. Age-related muscle deconditioning and weakening are associated with loss of muscle quality and quantity manifested as a decrease in muscle mass and the number of fibers, and altered myofibrillar protein expression.[26] Therefore, this animal histology study aimed to observe these indices as the main markers for successful treatment of the deconditioned muscle tissue.

Throughout the study, the active group showed significant improvement in all measurements. The overall muscle mass increased by 19.2% at a 2-month follow-up, which may be attributed to the densification of muscle fibers while they increased in diameter at the same time (Figure 4). There is evidence that an increase in muscle mass is correlated with higher muscle strength and function.[27] Such changes can have beneficial implications when it comes to the treatment of human patients and restoration of facial appearance, which relies on the functional muscle tissue that interconnects with the skin. Also, the increased muscle mass indicates the substitution of adipose and connective tissue with muscle tissue (Figure 5), accompanied by muscle fiber growth both in size (+15.9%) and quantity (+19.8%). In human patients, studies have shown that the increase in muscle thickness in the crosswise direction induced by facial exercise has a positive effect on facial rejuvenation because it contributes to firmer and more elastic facial skin with a decrease in mimetic muscles linked to sagging of the face.[28,29] Therefore HIFES facial therapy might provide a first attempt standardized facial protocol to mitigate the loss of bulk and lift in facial aging, as a postoperative treatment or a stand-alone regimen.

The last marker of the changes occurring in the muscle tissue during the study period was the number of myonuclei, which correlates with the size of muscle fibers.[30] The significant increase in the number of myonuclei (+21.2%) may be attributed to satellite cells, which are activated during exercise.[31,32] Because supramaximal muscle stimulation is an effective alternative to exercise, these satellite cells fuse with the muscle fibers and donate their nucleus to the fiber to increase the regenerative and remodeling responses of the muscle fibers.[32–34]

The mild difference in the number of muscle fibers observed at 1-month follow-up when compared to control is most likely due the short observation period. As Kadi et al showed in their review, the effects of satellite cell activation take approximately 50-90 days to propagate fully, which corresponds to our 2-month follow-up observation, when the increase of muscle fibers was found to be highly significant when compared to the control group (P value = .004).[35] Nonetheless, all markers increased gradually in the active group and no significant changes were observed in the control group, and we can attribute the results seen in the active group to the HIFES + RF sessions.

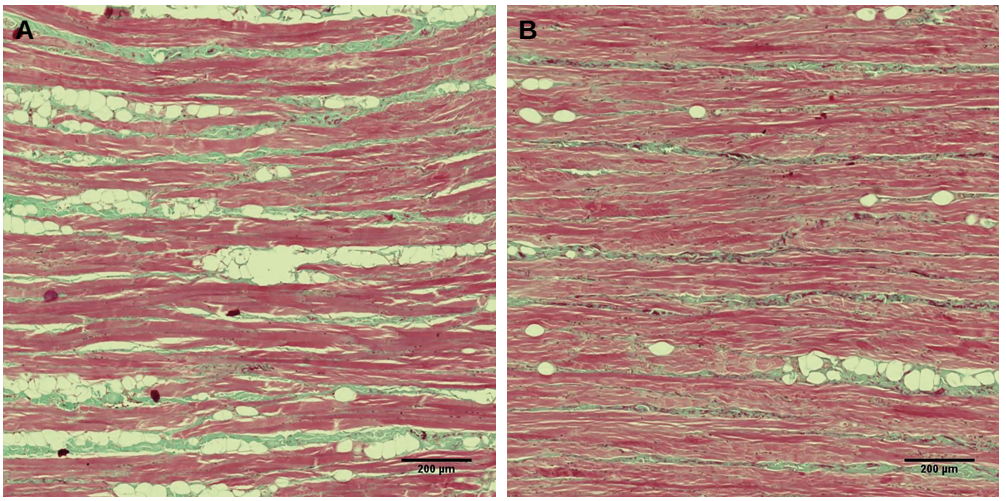

Figure 5. A longitudinal view of the muscle tissue stained by Masson's trichrome, taken at (A) baseline and (B) 2-month follow-up. The red color represents the muscle tissue, whereas the green color documents the presence of the intersected collagen fibers with lipid droplets without color. At baseline, the muscle fibers were relatively sparsely distributed, which changed at the 2-month follow-up. There was a noticeable increase in muscle fiber density together with a decrease in the fat tissue infiltration.

One of the limitations of this study was the use of a porcine animal model instead of human patients. Nonetheless, given the invasive nature of the study procedures, this animal model was found most suitable for the purpose of this study. Pigs have been successfully employed in biomedical research because of their remarkable similarity to humans in anatomy, physiology, immune system, and genome. These similarities provide sufficient insight to consider the biological processes transferable to humans.[36] Another limitation was the treatment area. Although the novel HIFES technology was designed to target all facial muscles, the trial was conducted on the pigs' foreheads only. The sow's cheek area was found to be problematic in terms of applicator placement and biopsy acquisition. However, the forehead area was eligible for treatments, because sow's forehead muscles are not intensively used by the animals, and therefore may correspond with deconditioned human muscles in the face. Also, all procedures were undertaken in a way to minimize animals' suffering. Taking samples from muscles of mastication in pigs may lead to pain during feeding and loss of appetite, resulting in weight loss and compromising the long-term results of the experiment. Nonetheless, we believe that the obtained results can be applied generally to the facial muscle groups because they all are subject to the same processes of deterioration.[37] Regarding the length of the follow-up, the animals were not kept with the general population, to lower the chances of infection or injury and overall bias from keeping them in uncontrolled conditions. Due to a long isolation with only study animals stress was considered a potential risk factor, and so there are no data available later than 2-month follow-up. This study was designed to investigate the immediate to short-term response of the tissue, and the 2-month period was deemed sufficient. The study's focus was to provide a basic understanding of the induced changes, which might provide insight into the effects of the simultaneous use of the investigated technologies with implications for use in human patients. In total, there were 144 evaluated tissue slices in this study, ensuring a reliable data count for conducted statistics. Also, 4 different aspects characterizing changes at the muscle tissue composition level were assessed, providing a comprehensive description of the effects of the investigated technology. In sum, this study offers a new method of noninvasive facial rejuvenation with the potential to contribute to the understanding of facial muscle aging in further detail. Future studies will benefit from using human patients to verify the findings described, and utilizing more objective methods (such as ultrasound) for a comprehensive analysis of the events occurring in the facial muscle tissue related to facial rejuvenation. Future human studies of a noninvasive nature should also consider including muscle testing of facial muscles to measure the improvement of facial expressions after the treatments, while establishing a longer follow-up period to document the long-term effects of the procedure.

CONCLUSIONS

This animal histology study aimed to evaluate the effectiveness and safety of the simultaneous application of novel HIFES technology and synchronized radiofrequency. The results documented by the histological analysis indicate

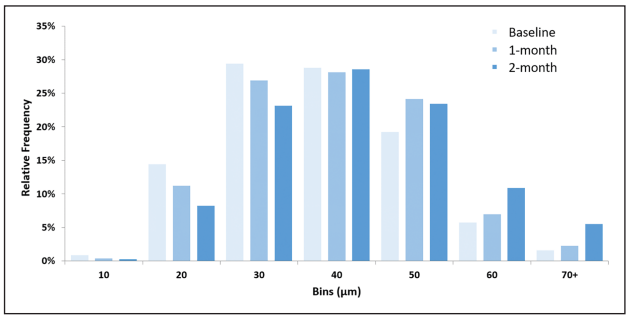

Figure 6. The histogram represents the relative frequency distribution of the muscle fiber sizes in the active group samples. The interval width was chosen to be 10 µm. The muscle fibers of greater diameters were more frequently present at 2-month follow-up.

treatment effectiveness for improving overall muscle quality; the active group significantly improved in all studied parameters. The safe use of this technology was also documented. No adverse effects occurred, and there were no unusual findings when assessing histology samples.

Disclosures

Drs Kinney and Bernardy are clinical investigators for BTL Industries (Boston, MA). Dr Jarošová is an associate of the Veterinary Research Institute (Brno, Czech Republic).

Funding

BTL Industries (Boston, MA) was the sponsor of this study and provided the study device. However, no funding for authorship and publication of this article was provided.

REFERENCES

1. Cotofana S, Assemi-Kabir S, Mardini S, et al. Understanding facial muscle aging: a surface electromyography study. *Aesthet Surg J*. 2021;41(9):NP1208-NP1217. doi: 10.1093/asj/sjab202
2. Swift A, Liew S, Weinkle S, Garcia JK, Silberberg MB. The facial aging process from the "inside out." *Aesthet Surg J*. 2021;41(10):1107-1119. doi: 10.1093/asj/sjaa339
3. Gupta MA, Gilchrest BA. Psychosocial aspects of aging skin. *Dermatol Clin*. 2005;23(4):643-648. doi: 10.1016/j.det.2005.05.012
4. Cotofana S, Fratila AAM, Schenck TL, Redka-Swoboda W, Zilinsky I, Pavicic T. The anatomy of the aging face: a review. *Facial Plast Surg*. 2016;32(3):253-260. doi: 10.1055/s-0036-1582234
5. Volpi E, Nazemi R, Fujita S. Muscle tissue changes with aging. *Curr Opin Clin Nutr Metab Care*. 2004;7(4):405-410. doi: 10.1097/01.mco.0000134362.76653.b2
6. Evans WJ. Skeletal muscle loss: cachexia, sarcopenia, and inactivity. *Am J Clin Nutr*. 2010;91(4):1123S-1127S. doi: 10.3945/ajcn.2010.28608A
7. Salari M, Sharma S, Jog MS. Botulinum toxin induced atrophy: an uncharted territory. *Toxins (Basel)*. 2018;10(8):313. doi: 10.3390/toxins10080313
8. Durand PD, Couto RA, Isakov R, et al. Botulinum toxin and muscle atrophy: a wanted or unwanted effect. *Aesthet Surg J*. 2016;36(4):482-487. doi: 10.1093/asj/sjv208
9. Westbrook KE, Nessel TA, Hohman MH, Varacallo M. *Anatomy, Head and Neck, Facial Muscles*. StatPearls Publishing; 2021. Accessed April 5, 2022. https://www.ncbi.nlm.nih.gov/books/NBK493209
10. Jacob C, Kent D, Ibrahim O. Efficacy and safety of simultaneous application of HIFEM and synchronized radiofrequency for abdominal fat reduction and muscle toning: a multicenter magnetic resonance imaging evaluation study. *Dermatol Surg*. 2021;47(7):969-973. doi: 10.1097/DSS.0000000000003086
11. Kar BR, Ray A. Cosmetic dermatologic surgery abstracts. Published February 22, 2021. Accessed April 13, 2022. https://www.asds.net/portals/0/PDF/am21-abstracts.pdf
12. Palm M, Kinney B, Halaas Y, Goldfarb R. ASLMS 2021 Abstracts. *Lasers Surg Med*. 2021;53(S33):S5-S49. doi: 10.1002/lsm.23409
13. Chen I, Lui F. *Neuroanatomy, Neuron Action Potential*. StatPearls Publishing; 2021. Accessed April 6, 2022. https://www.ncbi.nlm.nih.gov/books/NBK546639
14. Slater CR. The structure of human neuromuscular junctions: some unanswered molecular questions. *Int J Mol Sci*. 2017;18(10):2183. doi: 10.3390/ijms18102183
15. McGorm H, Roberts L, Coombes J, Peake J. Turning up the heat: an evaluation of the evidence for heating to promote exercise recovery, muscle rehabilitation and adaptation. *Sports Med*. 2018;48(6):1311-1328. doi: 10.1007/s40279-018-0876-6
16. Dayan E, Burns AJ, Rohrich RJ, Theodorou S. The use of radiofrequency in aesthetic surgery. *Plast Reconstr Surg Glob Open*. 2020;8(8):e2861. doi: 10.1097/GOX.0000000000002861
17. Mehta-Ambalal SR. Neocollagenesis and neoelastinogenesis: from the laboratory to the clinic. *J Cutan Aesthet Surg*. 2016;9(3):145-151. doi: 10.4103/0974-2077.191645
18. Avwioro G. Histochemical uses of haematoxylin—a review. *JPCS*. 2010;1:24-34.
19. Chan JKC. The wonderful colors of the hematoxylin–eosin stain in diagnostic surgical pathology. *Int J Surg Pathol*. 2014;22(1):12-32. doi: 10.1177/1066896913517939
20. Fisher AH, Jacobson KA, Rose J, Zeller R. Hematoxylin and eosin staining of tissue and cell sections. *CSH Protoc*. 2008;2008:pdb.prot4986. doi: 10.1101/pdb.prot4986
21. Wang C, Yue F, Kuang S. Muscle histology characterization using H&E staining and muscle fiber type classification using immunofluorescence staining. *Bio Protoc*. 2017;7(10):e2279. doi: 10.21769/BioProtoc.2279
22. Mokobi F. Masson's trichrome staining. Microbe notes. Published October 28, 2020. Accessed April 13, 2022. https://microbenotes.com/massons-trichrome-staining
23. Al-Mahmood SS. Improving light microscopic detection of collagen by trichrome stain modification. *Iraqi J Vet Sci*. 2020;34(2):273-281. doi: 10.33899/ijvs.2019.126176.1256

24. Assaw S. The use of modified Massion's trichrome staining in collagen evaluation in wound healing study. *Malaysian J Vet Res*. 2012;3:39-47.
25. Mao H, Su P, Qiu W, Huang L, Yu H, Wang Y. The use of Masson's trichrome staining, second harmonic imaging and two-photon excited fluorescence of collagen in distinguishing intestinal tuberculosis from Crohn's disease. *Colorect Dis*. 2016;18(12):1172-1178. doi: 10.1111/codi.13400
26. Cristea A, Qaisar R, Edlund PK, Lindblad J, Bengtsson E, Larsson L. Effects of aging and gender on the spatial organization of nuclei in single human skeletal muscle cells. *Aging Cell*. 2010;9(5):685-697. doi: 10.1111/j.1474-9726.2010.00594.x
27. Reed RL, Pearlmutter L, Yochum K, Meredith KE, Mooradian AD. The relationship between muscle mass and muscle strength in the elderly. *J Am Geriatr Soc*. 1991;39(6):555-561. doi: 10.1111/j.1532-5415.1991.tb03592.x
28. Lim H. Effects of facial exercise for facial muscle strengthening and rejuvenation: systematic review. *J Korean Phys Ther*. 2021;33(6):297-303. doi: 10.18857/jkpt.2021.33.6.297
29. Hwang UJ, Kwon OY, Jung SH, Ahn SH, Gwak GT. Effect of a facial muscle exercise device on facial rejuvenation. *Aesthet Surg J*. 2018;38(5):463-476. doi: 10.1093/asj/sjx238
30. Ato S, Ogasawara R. The relationship between myonuclear number and protein synthesis in individual rat skeletal muscle fibres. *J Exp Biol*. 2021;224(10):jeb242496. doi: 10.1242/jeb.242496
31. Kaczmarek A, Kaczmarek M, Ciałowicz M, et al. The role of satellite cells in skeletal muscle regeneration—the effect of exercise and age. *Biology (Basel)*. 2021;10(10):1056. doi: 10.3390/biology10101056
32. Karatzanos E, Gerovasili V, Zervakis D, et al. Electrical muscle stimulation: an effective form of exercise and early mobilization to preserve muscle strength in critically ill patients. *Crit Care Res Pract*. 2012;2012:432752. doi: 10.1155/2012/432752
33. Murach KA, Dungan CM, Peterson CA, McCarthy JJ. Muscle fiber splitting is a physiological response to extreme loading in animals. *Exerc Sport Sci Rev*. 2019;47(2):108-115. doi: 10.1249/JES.0000000000000181
34. Snijders T, Nederveen JP, McKay BR, et al. Satellite cells in human skeletal muscle plasticity. *Front Physiol*. 2015;6:283. doi: 10.3389/fphys.2015.00283
35. Kadi F, Charifi N, Denis C, et al. The behaviour of satellite cells in response to exercise: what have we learned from human studies? *Pflugers Arch*. 2005;451(2):319-327. doi: 10.1007/s00424-005-1406-6
36. Lunney JK, Van Goor A, Walker KE, Hailstock T, Franklin J, Dai C. Importance of the pig as a human biomedical model. *Sci Transl Med*. 2021;13(621):eabd5758. doi: 10.1126/scitranslmed.abd5758
37. Mok GF, Sweetman D. Many routes to the same destination: lessons from skeletal muscle development. *Reproduction*. 2011;141(3):301-312. doi: 10.1530/REP-10-0394